A Fourth-Order in Space and Second-Order in Time TLM Model

N. R. S. Simons, *Member, IEEE,* and A. Sebak, *Senior Member, IEEE*

Abstract— **In this paper a new TLM model is presented for solving two-dimensional electromagnetic field problems. The new model possesses the same dispersion relation as a fourth-order in space and second-order in time central-finite-difference algorithm. The stability criterion of the TLM model (given in terms of permissible values for the admittance of the permittivity stub) is provided. Investigation of the propagation characteristics indicates the benefits of fourth-order spatial discretization, especially for modelling dielectric media. The improved dispersive properties of the fourth-order models make them attractive candidates for the analysis of electrically large (and inhomogeneous) problems. The scattering and transfer events for the new model are presented as well as results from numerical experiments. The improved computational efficiency of the new fourth-order accurate model in terms of both memory storage and computation time (as compared to the original second-order TLM algorithm) is demonstrated.**

I. Introduction

THE Transmission-Line Matrix (TLM) method is capable of providing an approximate solution to the time-dependent form of Maxwell's equations in arbitrary media [1], [2]. For this reason the method is considered to be in the same class as time-domain finite-difference and finite-element methods. The finite-difference and finite-element methods are general techniques applicable to the numerical solution of differential equations [3]. Both methods allow flexibility in the geometrical properties of the numerical grid and the order of accuracy of the governing approximation. The finite-difference method allows various spatial arrangements of the difference approximations and different orders of accuracy. The finite-element method allows various element shapes and element expansion functions of varying order. In two previous papers [4], [5], TLM models have been presented on two types of triangular grids: an equilateral triangular grid in [4], which is referred to as the hexagonal TLM model, and an isosceles triangular grid in [5] which is referred to as the spatially weighted TLM model. Both the hexagonal and spatially weighted models indicate the ability of the TLM approach to make use of numerical grids that are different from the traditional rectangular approach. In this paper the extension of the original second-order accurate TLM model to achieve fourth-order spatial approximation is presented.

Numerical models for wave propagation represent a discretized medium that is both dispersive and anisotropic, i.e., the propagation velocity in the numerical mesh depends on both the frequency content of the signal and the direction of propagation. This undesired effect is referred to as velocity error and is determined from the dispersion relation for the particular model. Velocity error is one possible source for errors that may arise in the practical application of the finite-difference, finite-element, or TLM methods. The benefit of the models presented in [4] and [5] is that approximate numerical isotropy is obtained. In [4] an error-correction procedure is presented for reducing dispersive errors when approximate numerical isotropy is achieved. The fundamental accuracy of all three models is second-order in both space and time. Only the number, spatial orientation, and relative weighting of the difference approximations are distinct. While the previously developed models investigate improvements to the anisotropy of the numerical model, the purpose of the present investigation is to investigate possible improvements to the frequency dependence of the numerical model through extension of the original second-order algorithm to achieve fourth-order spatial accuracy.

The present investigation makes use of the dispersive equivalence of TLM and finite-difference methods previously described in [4]–[6]. A dispersive equivalence exists between two numerical methods if both possess identical dispersion relations. Dispersive equivalence does not involve the definition of field quantities, operation of the algorithm, or application of boundary conditions. For existing two-dimensional TLM models (the original rectangular [7], the hexagonal [4], and the spatially weighted model [5]), a dispersive equivalence exists with a second-order in time and second-order in space central-difference approximation of the two-dimensional wave equation. The differences between the three models is the manner in which the second-order finite-difference operator is applied to the spatial derivatives. The application of higher-order approximations to time-domain differential-equation based numerical methods (either finite-difference or finite-element) has received limited attention. Fang and Mei [8], and Deveze *et al.* [9] have investigated the use of higher-order accurate finite-difference algorithms.

In the following section a fourth-order in space and second-order in time finite-difference algorithm is presented. The dispersion relation and stability criteria for this algorithm are derived. In Section III, the fourth-order in space and

Manuscript received October 11, 1993; revised May 20, 1994. This work was supported by the Natural Sciences and Engineering Research Council of Canada and MICRONET.

N. R. S. Simons was with InfoMagnetics Technologies Corporation, Winnipeg, Manitoba, Canada. He is now with the Directorate of Antennas and Integrated Electronics, Communiations Research Centre, Ottawa, Ontario, Canada.

A. Sebak is with the Department of Electrical and Computer Engineering, University of Manitoba, Winnipeg, Manitoba R3T 2N2, Canada.

IEEE Log Number 9407303.

second-order in time TLM model is presented. This model is synthesized directly from the finite-difference algorithm. The dispersion relation for the TLM model is derived and its equivalence with the finite-difference dispersion relation is discussed. In Section IV, the propagation characteristics of the fourth-order in space and second-order in time algorithms are evaluated and compared to those of the original TLM model. The results indicate the superior performance of the fourth-order models for the modelling of dielectric media. The scattering and transfer events required for the practical implementation of the TLM model are presented in Section V, as well as numerical examples presented for validation. In Section VI the computational benefits of fourth-order spatial discretization, in terms of cpu time and memory storage, are provided.

II. Finite-Difference Algorithm

In this paper, the finite-difference algorithms and the TLM models considered provide approximate solutions to the two-dimensional wave equation,

$$\frac{\partial^2 E}{\partial x^2} + \frac{\partial^2 E}{\partial y^2} = \frac{1}{c^2}\frac{\partial^2 E}{\partial t^2} \tag{1}$$

where E is the z directed electric field distribution ($E = E(x, y, t)$), and v is the propagation velocity. Consider the discretization of (1) using fourth-order central-difference approximations in space and a second-order central-difference approximation in time, to yield

$$\begin{aligned}&\left(-E^t(x+2\Delta l, y) + 16E^t(x+\Delta l, y) - 30E^t(x,y)\right.\\&\quad\left. + 16E^t(x-\Delta l.y) - E^t(x-2\Delta l, y)\right)/12(\Delta l)^2\\&\quad + \left(-E^t(x, y+2\Delta l) + 16E^t(x, y+\Delta l) - 30E^t(x,y)\right.\\&\quad\left. + 16E^t(x, y-\Delta l) - E^t(x, y-2\Delta l)\right)/12(\Delta l)^2\\&\qquad = \frac{1}{v^2}\frac{E^{t+\Delta t}(x,y) - 2E^t(x,y) + E^{t-\Delta t}(x,y)}{(\Delta t)^2}\end{aligned} \tag{2}$$

where Δl is the grid size in the x and y directions, and Δt is the time step. Following [10], the dispersion relation of the finite-difference algorithm (2) is,

$$\begin{aligned}&-\sin^2(\beta^*\Delta l\cos\phi) - \sin^2(\beta^*\Delta l\sin\phi)\\&\quad + 16\sin^2\left(\frac{\beta^*\Delta l\cos\phi}{2}\right) + 16\sin^2\left(\frac{\beta^*\Delta l\sin\phi}{2}\right)\\&\qquad = \frac{12\Delta l^2}{v^2\Delta t^2}\sin^2\left(\frac{\omega\Delta t}{2}\right)\end{aligned} \tag{3}$$

Equation 3 describes the fundamental manner in which plane waves propagate through a finite-difference mesh of infinite extent. Given the spatial Δl and temporal discretization Δt, respectively, frequency of excitation ω, direction of propagation ϕ, the numerical phase constant β^* can be obtained from (3). The value of β^* can be compared to the exact physical phase constant β to determine the amount of velocity error.

The stability criterion for the spatially fourth-order finite-difference algorithm determined using the Von Neumann method [11] is

$$\Delta t \le \sqrt{\frac{3}{8}}\,\frac{\Delta l}{v} \tag{4}$$

The maximum allowable Courant number for (2) is $\sqrt{(3/8)}$, where the Courant number is defined as $v\Delta t/\Delta l$ [10].

The Yee finite-difference time-domain algorithm [12], [13] is obtained from discretization of Maxwell's curl equations using second-order central-difference approximations in both space and time. The Yee algorithm can be re-written in terms of only the electric field values at even space and time steps. In two dimensions the equivalent algorithm in terms of only electric field values is expressed as,

$$\begin{aligned}&\frac{E^t(x+\Delta l, y) - 2E^t(x,y) + E^t(x-\Delta l, y)}{(\Delta l)^2}\\&\quad + \frac{E^t(x, y+\Delta l) - 2E^t(x,y) + E^t(x, y-\Delta l)}{(\Delta l)^2}\\&\quad = \frac{1}{v^2}\frac{E^{t+\Delta t}(x,y) - 2E^t(x,y) + E^{t-\Delta t}(x,y)}{(\Delta t)^2}\end{aligned} \tag{5}$$

The memory storage requirements of the fourth-order in space and second-order in time algorithm (2) and the second-order in both space and time algorithm (5) are identical. However, the fourth-order in space and second-order in time algorithm (2) requires more computation per time step than the second-order algorithm (5).

III. Synthesis of TLM Model

The spatially fourth-order TLM model is synthesized directly from the finite difference algorithm (2). The synthesis closely follows that of the spatially weighted TLM model [5]. The propagation velocities of the elemental transmission lines are selected to mimic the propagation of information within the finite-difference algorithm, and the intrinsic impedances of the elemental transmission lines are selected to provide appropriate weighting between the analogous finite-difference operators.

The fourth-order central-difference operator can be expressed in terms of two second-order operators,

$$\frac{\partial^2 f}{\partial \eta^2} \approx \frac{4}{3}D_{\Delta l}f - \frac{1}{3}D_{2\Delta l}f \tag{6}$$

where,

$$D_h f = \frac{f(\eta+h) - 2f(\eta) + f(\eta-h)}{h^2}$$

One operator has a weight 4/3 and operates on a $1\Delta l$ grid; the other has a weight $-1/3$ and operates on a 2Δ l grid. The spatially fourth-order TLM model is constructed from the interconnection of two original models, one with a mesh spacing of Δl, the other with a mesh spacing $2\Delta l$. A mesh of fourth-order TLM nodes is provided in Fig. 1, and an individual node is provided in Fig. 2. The required weighting is accomplished by the different intrinsic impedances (Z_l for elemental transmission lines 1–4 and $-16Z_l$ for elemental transmission lines 5–8), and preservation of the speed of information transfer is accommodated using different propagation velocities (v_l for elemental transmission lines 1–4 and $2v_l$ for elemental transmission lines 5–8). At all nodal locations, eight elemental transmission lines intersect. These lines connect a node $(n\Delta l, m\Delta l)$ to nodes

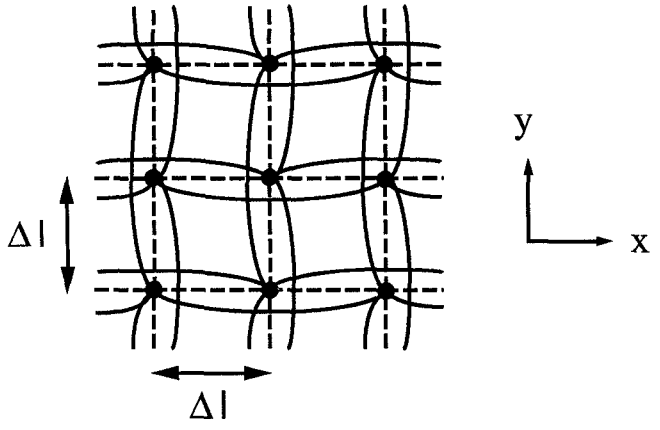

Fig. 1. Mesh of fourth-order TLM nodes.

$((n \pm 1)\Delta l, m\Delta l), ((n \pm 2)\Delta l, m\Delta l), (n\Delta l, (m \pm 1)\Delta l)$, and $(n\Delta l, (m \pm 2\Delta l)$, where n and m are integers describing an arbitrary spatial location in the mesh. Essentially, nodes separated by a distance Δl (in the x and y directions) are directly connected by an elemental transmission-line of intrinsic impedance Z_l and propagation velocity v_l. Nodes separated by a distance $2\Delta l$ (in the x and y directions) are directly connected by an elemental transmission-line of intrinsic impedance $-16Z_l$ and propagation velocity $2v_l$. As presented in [5], two permittivity stubs are used. One is of length $\Delta l/2$, with propagation velocity v_l, and admittance Y_0/Z_l; the other of length Δl, with propagation velocity $2v_l$, and admittance $-Y_0/16Z_l$. The complete fourth-order TLM node, with a description of the electrical properties of the elemental transmission lines, is provided in Fig. 2.

Following the procedure described in [14] the dispersion relation of the fourth-order TLM model is given by,

$$\begin{aligned} &-\sin^2(\beta^*\Delta l\cos\phi) - \sin^2(\beta^*\Delta l\sin\phi) \\ &\quad + 16\sin^2\left(\frac{\beta^*\Delta l\cos\phi}{2}\right) + 16\sin^2\left(\frac{\beta^*\Delta l\sin\phi}{2}\right) \\ &\quad = \left(30 + \frac{15}{2}Y_0\right)\sin^2\left(\frac{\omega\Delta t}{2}\right) \end{aligned} \tag{7}$$

Expression 7 describes the fundamental manner in which plane waves propagate through an infinite mesh of fourth-order TLM nodes.

Several investigations regarding the algorithmic equivalence of TLM and finite-difference methods have been performed [15]: partial algorithmic equivalence of the three-dimensional expanded TLM model with the three-dimensional Yee finite-difference time-domain algorithm [15]; partial algorithmic equivalence of the original two-dimensional TLM model with the two-dimensional Yee algorithm [16]; and complete algorithmic equivalence of the original two-dimensional TLM model and the three-dimensional symmetric-condensed TLM model with new finite-difference time-domain algorithms [17]. In [4]–[6] dispersive equivalences of the original-rectangular, hexagonal, and spatially weighted TLM models to second-order (in both space and time) finite-difference algorithms are provided. Both types of equivalence (algorithmic and dispersive) help to establish the order of accuracy of a given TLM model through equivalence with a specific finite-difference algorithm.

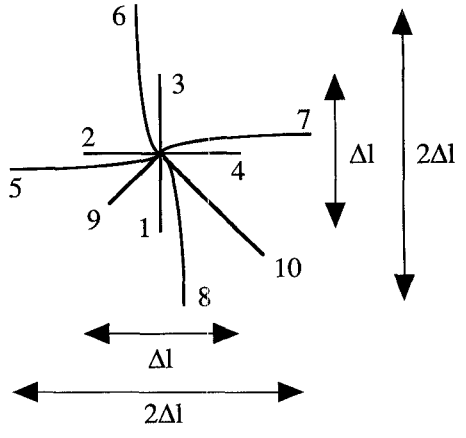

Fig. 2. An individual fourth-order TLM node with permittivity stubs for-modelling an arbitrary dielectric material.

Consider a mesh of fourth-order TLM models with a specific value of permittivity stub Y_0. If the finite-difference algorithm (2) is operated such that Δl and Δt satisfy,

$$v = \sqrt{\frac{24}{60 + 15Y_0}}\frac{\Delta l}{\Delta t} \tag{8}$$

(3) and (7) are identical, and therefore the fourth-order finite-difference algorithm and TLM model possess identical dispersion relations. From the finite-difference stability criterion (4), the permissible range of values for the stub admittance Y_0 (the stability criterion for the fourth-order TLM model) is given by,

$$Y_0 \geq \frac{4}{15} \tag{9}$$

Selecting $Y_0 = 4/15$ to represent a free-space medium, the relationship between the permittivity value and the relative dielectric constant of the medium modelled by a mesh of fourth-order nodes is,

$$\varepsilon_r = \frac{60 + 15Y_0}{64} \tag{10}$$

For certain positive stub values (i.e., $0 \leq Y_0 < 4/15$) the fourth-order model is unstable. This instability for a range of positive Y_0 is unique to the fourth-order model. All previously investigated second-order algorithms [4], [5], [7] are stable for $Y_0 \geq 0$.

IV. Evaluation of Propagation Characteristics

In Fig. 3, the propagation characteristics of the original TLM model [7] and the spatially fourth-order model are compared for propagation along a coordinate direction. The two curves are provided at the upper limit of stability (i.e., $Y_0 = 0$ for the original algorithm and $Y_0 = 4/15$ for the fourth-order algorithm). Two benefits of the fourth-order model are evident. The first benefit is the improved accuracy

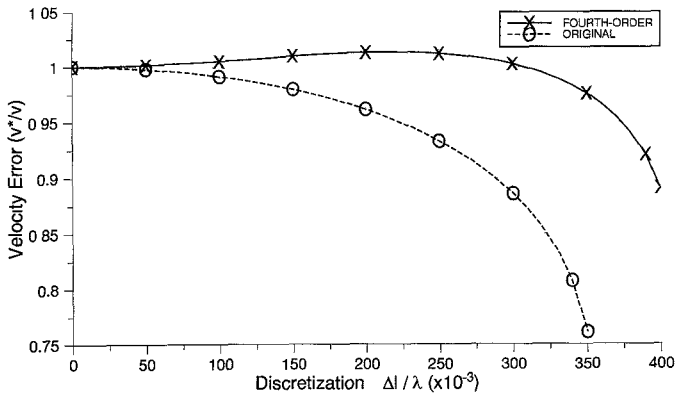

Fig. 3. Velocity error v^*/v versus $\Delta l/\lambda$ for the original model [7] and the spatially fourth-order model for propagation along a coordinate direction (both algorithms operated at their respective stability limits)

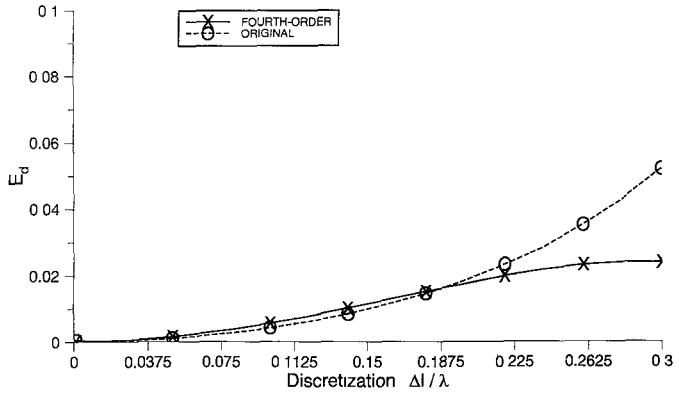

Fig. 4. Error E_d versus $\Delta l/\lambda$ for the original and fourth-order TLM models (both algorithms operated at their respective stability limits).

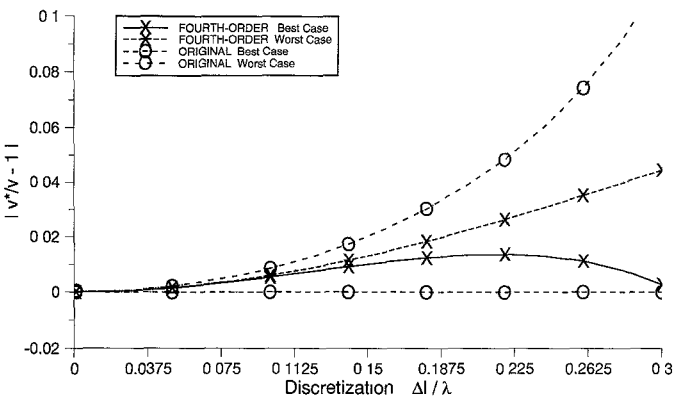

Fig. 5. Minimum and maximum values for $|(v^*/v)-1|$ versus $\Delta l/\lambda$ for the original and fourth-order TLM models. The minimum and maximum values of $|(v^*/v)-1|$ for the original algorithm occur for propagation in the $\phi = 45°$ and $\phi = 0°$ directions. The minimum and maximum values of $|(v^*/v)-1|$ for the fourth-order algorithm occur for propagation in the $\phi = 0°$ and $\phi = 45°$ directions.

of the fourth-order model. The second benefit is the increase in cut-off frequency provided by the fourth-order model.

The propagation characteristics of the fourth-order model display different behavior than the second-order models. The second-order models [4], [5], [7] simulate a medium in which the propagation velocity is too slow, $v^*/v \leq 1.0$. At the limit of stability and for fine spatial discretization, the fourth-order model simulates a medium in which the propagation velocity is too fast, $v^*/v \geq 1.0$, and for frequencies near cut-off, the fourth-order model simulates a medium in which the propagation velocity is too slow. For propagation along a mesh axis, the accuracy of the fourth-order model is always superior to the original model.

To gain more insight into the relative performance of the original and fourth-order algorithms, consider the following measure of error for characterizing the various algorithms:

$$E_d\left(\frac{\Delta l}{\lambda}\right) = \frac{1}{360}\sum_{\phi=0°}^{360°}\left|\left(\frac{v^*}{v}\right)_{\frac{\Delta l}{\lambda}} - 1\right| \qquad (11)$$

The value of $E_d(\Delta l/\lambda)$ will provide a measure of the dispersive errors at a given discretization $(\Delta l/\lambda)$ averaged over all directions of propagation. Therefore, E_d does not provide information regarding the anisotropy of the model. This measure is perhaps more relevant for general problems (in which wave propagation takes place in a variety of different directions) rather than investigating the propagation characteristics for specific directions of propagation. Also, note the normalization factor and the upper limit of the summation can be reduced from 360° to 90° due to the rotational symmetry of the models considered in this paper.

In Fig. 4, the values of E_d are provided for the original and fourth-order models versus $\Delta l/\lambda$. This figure indicates that for $\Delta l/\lambda \leq 0.1875$ the original algorithm possesses a slightly lower value of E_d than the fourth-order algorithm. This unexpected result is due to the perfect propagation that occurs in the original algorithm for propagation diagonally through the mesh. In Fig. 5, the best and worst case values of $|(v^*/v) - 1|$ are provided versus $\Delta l/\lambda$. The value for E_d can be approximately considered as the average between these minimum and maximum values of $|(v^*/v) - 1|$. Fig. 5 indicates that the maximum value of $|(v^*/v) - 1|$ for the original model (which occurs for propagation along one of the coordinate directions) is larger than the maximum value for the fourth-order algorithm (which occurs for propagation diagonally through the mesh). However, the minimum value of $|(v^*/v) - 1|$ for the original algorithm is zero (because this algorithm provides dispersionless propagation with infinite cut-off for $\phi = 45°$), and therefore superior to the direction with the minimum value of $|(v^*/v) - 1|$ for the fourth-order algorithm. Since E_d is approximately the average of the minimum and maximum values of $|(v^*/v) - 1|$, Figs. 4 and 5 indicate that the original algorithm is slightly better than the fourth-order algorithm for $\Delta l/\lambda \leq 0.1875$. The fourth-order algorithm is superior for $\Delta l/\lambda \leq 0.1875$.

In Fig. 6, the values of E_d for the original and fourth-order algorithms are compared for the case of modelling a dielectric material of $\varepsilon_r = 4$. These results indicate superior performance of the fourth-order algorithm. In fact, for increasing values of ε_r, the dispersive errors of the fourth-order algorithm decrease (for small values of $\Delta l/\lambda$). In Fig. 7, E_d is provided versus $\Delta l/\lambda_d$ for $\varepsilon_r = 1$, 2, 10, and 25. The results of this figure indicate that for typical practical discretizations $\Delta l/\lambda < 0.10$ the value of E_d decreases with increasing ε_r. This aspect of the behavior of the fourth-order model is distinct from the second-

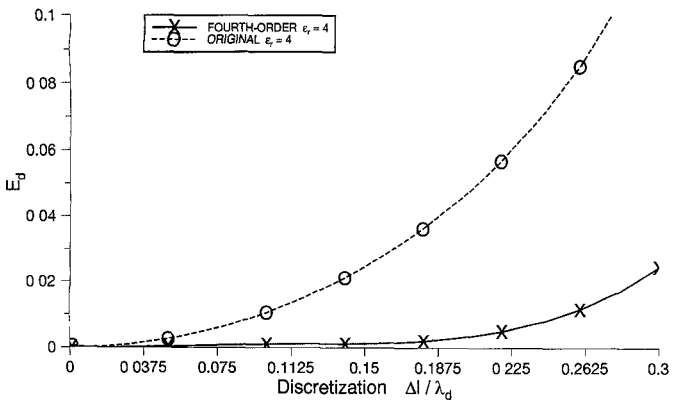

Fig. 6. Error E_d versus $\Delta l/\lambda$ for the original and fourth-order TLM models for the case of modelling a dielectric material of $\varepsilon_r = 4$.

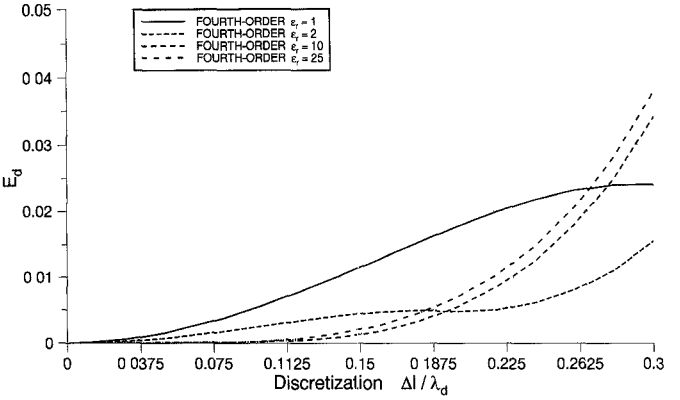

Fig. 7. Error E_d versus $\Delta l/\lambda$ for the fourth-order TLM model for modelling a dielectric material of $\varepsilon_r = 1, 2, 10$, and 25.

order models. In the equivalent finite-difference algorithms, the effect of increasing ε_r is equivalent to decreasing the Courant number. For the second-order algorithms, it is always desirable to run simulations at (or very close to) the Courant number, where the optimal propagation characteristics are obtained. This is not the case for the fourth-order algorithm presented in this paper. For this reason it may be desirable to renormalize the algorithm for a value of $Y_0 > 4/15$ to represent a free-space medium such that the optimal propagation characteristics of the fourth-order algorithm can be exploited.

In Fig. 8 the propagation characteristics of the original TLM model [7] and the spatially fourth-order model are compared for propagation along a coordinate direction in a medium with $\varepsilon_r = 10$. These curves indicate the superior performance of the fourth-order algorithm for the modelling of dielectric media (for a specific direction of propagation). The results indicate the fourth-order algorithm produces less than one percent velocity error for $\Delta l/\lambda < 0.2$. Velocity errors compound for waves which propagate over electrically large distances due to phase errors, which increase linearly with the distance travelled. Therefore, the potential benefits of fourth-order algorithms may become important for the analysis of electrically large problems.

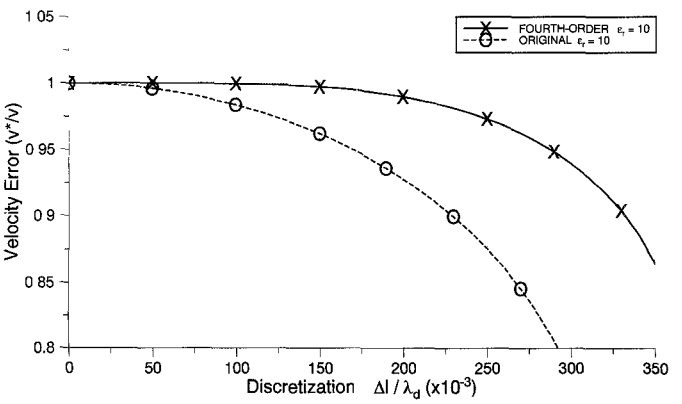

Fig. 8. Velocity error v^*/v versus $\Delta l/\lambda$ for the original model [7] and the spatially fourth-order model for propagation along a coordinate direction in a medium $\varepsilon_r = 10$.

V. Implementation—Scattering and Transfer Events

TLM algorithms operate by simulating the progression of voltage pulses as they are scattered through the mesh of transmission lines. The implementation of the spatially fourth-order model follows the same procedure as all other TLM models, i.e., scattering of incident voltage pulses at the junction of transmission lines and the transfer of reflected voltage pulses to adjacent nodes [1], [2].

The nodal scattering matrix for the spatially fourth-order TLM model is assembled by examining the reflection and transmission coefficients of a voltage pulse on each of the ten elemental transmission lines. For example, a voltage pulse approaching the transmission-line junction on branch 1 (a Z_l transmission-line) *sees* a parallel connection of three Z_l lines, four $-16Z_l$ lines, one Z_l/Y_0 line, and one $-16Z_l/Y_0$ line. The corresponding reflection coefficient (describing the magnitude of the voltage pulse reflected from the transmission-line junction back onto line 1) is,

$$\Gamma = \frac{\left(\frac{3}{Z_l} - \frac{4}{16Z_l} + \frac{Y_0}{Z_l} - \frac{Y_0}{16Z_l}\right)^{-1} - Z_l}{\left(\frac{3}{Z_l} - \frac{4}{16Z_l} + \frac{Y_0}{Z_l} - \frac{Y_0}{16Z_l}\right)^{-1} + Z_l} = \frac{\frac{16}{44+15Y_0} - 1}{\frac{16}{44+15Y_0} + 1} = \frac{-28 - 15Y_0}{60 + 15Y_0}$$

The corresponding transfer coefficient (describing the magnitude of the voltage pulse transmitted to the other nine transmission-line branches) is,

$$T = 1 + \Gamma = \frac{32}{60 + 15Y_0}$$

Following the above procedure, the complete nodal scattering matrix can be assembled:

$$\begin{bmatrix} v_1^r \\ v_2^r \\ v_3^r \\ v_4^r \\ v_5^r \\ v_6^r \\ v_7^r \\ v_8^r \\ v_9^r \\ v_{10}^r \end{bmatrix} = \begin{bmatrix} a & b & b & b & d & d & d & d & f & h \\ b & a & b & b & d & d & d & d & f & h \\ b & b & a & b & d & d & d & d & f & h \\ b & b & b & a & d & d & d & d & f & h \\ b & b & b & b & c & d & d & d & f & h \\ b & b & b & b & d & c & d & d & f & h \\ b & b & b & b & d & d & c & d & f & h \\ b & b & b & b & d & d & d & c & f & h \\ b & b & b & b & d & d & d & d & e & h \\ b & b & b & b & d & d & d & d & f & g \end{bmatrix} \begin{bmatrix} v_1^i \\ v_2^i \\ v_3^i \\ v_4^i \\ v_5^i \\ v_6^i \\ v_7^i \\ v_8^i \\ v_9^i \\ v_{10}^i \end{bmatrix} \quad (12)$$

where

$$a = -\frac{28 + 15Y_0}{60 + 15Y_0}$$
$$b = \frac{32}{60 + 15Y_0}$$
$$c = -\frac{62 + 15Y_0}{60 + 15Y_0}$$
$$d = -\frac{2}{60 + 15Y_0}$$
$$e = \frac{17Y_0 - 60}{60 + 15Y_0}$$
$$f = \frac{32Y_0}{60 + 15Y_0}$$
$$g = -\frac{60 + 17Y_0}{60 + 15Y_0}$$
$$h = -\frac{2Y_0}{60 + 15Y_0}$$

The transfer event for the fourth-order model is:

$$\begin{aligned} v_1^i(i,j) &= v_3^r(i,j-1) & v_2^i(i,j) &= v_4^r(i-1,j) \\ v_3^i(i,j) &= v_1^r(i,j+1) & v_4^i(i,j) &= v_2^r(i+1,j) \\ v_5^i(i,j) &= v_7^r(i,j-2) & v_6^i(i,j) &= v_8^r(i-2,j) \\ v_7^i(i,j) &= v_5^r(i,j+2) & v_8^i(i,j) &= v_6^r(i+2,j) \\ v_9^i(i,j) &= v_9^r(i,j) & v_{10}^i(i,j) &= v_{10}^r(i,j) \end{aligned}$$

where (i,j) denote discrete (x,y) coordinates.

In Section II it was noted that increasing the spatial accuracy from second- to fourth-order did not require an increase in memory storage requirements for the finite-difference algorithm. This is not true for the TLM model. The fourth-order TLM model requires twice the memory storage of the second-order TLM model. For both the fourth-order TLM and finite-difference algorithms, increasing the spatial accuracy from second to fourth-order requires more computation per time step.

The performance and stability of the spatially fourth-order model has been verified for various wave propagation problems. In Fig. 9, the improved propagation characteristics of the spatially fourth-order model are demonstrated. The fourth-order model and the original TLM model [7] are applied to the simulation of a Gaussian-pulsed plane wave. An effective one-dimensional simulation in the x direction is created by applying magnetic walls along the minimum and maximum y boundaries. The fourth-order model preserves the shape of the pulse more accurately than the original model. As well, the fundamental difference in the propagation characteristics provided in Fig. 3 is evident. The Gaussian pulse contains significant energy from $\Delta l/\lambda = 0$ to approximately 0.250. The dispersion caused by the original model is evident in the trailing edge of the pulse (i.e., certain components of the wave propagate too slow). The dispersion caused by the fourth-order model is evident in the leading edge of the pulse (i.e., certain components of the wave propagate too fast). This example illustrates the behavior described in Fig. 3.

In Fig. 10, the improved propagation characteristics of the fourth-order model for modelling dielectric media are demonstrated. The original and fourth-order models are applied to the simulation of a Gaussian-pulse plane wave in a medium with $\varepsilon_r = 10$. The results indicate the superior performance of the fourth-order model. The waveform is significantly distorted by the original model and only slightly distorted by the fourth-order model. The simulated results of Fig. 10 verify the behavior displayed in Fig. 8.

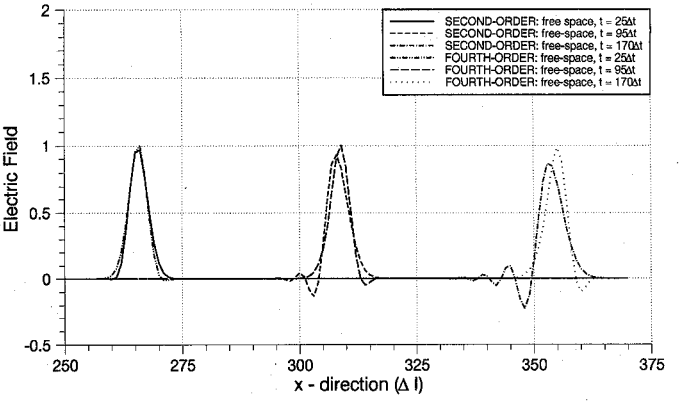

Fig. 9. Simulation of a Gaussian-pulsed plane wave by a mesh of original nodes [7], and a mesh of spatially fourth-order nodes.

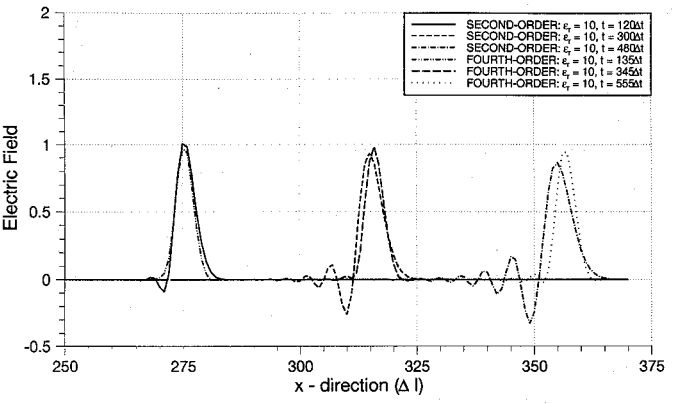

Fig. 10. Simulation of a Gaussian-pulsed plane wave in a medium with $\varepsilon_r = 10$ by a mesh of original nodes [7], and a mesh of spatially fourth-order nodes.

VI. Computational Efficiency

The dispersive analysis presented in Section IV, and the one-dimensional propagation examples provided in the previous section indicate the superior accuracy of the new fourth-order model. These examples do not, however, demonstrate the computational advantage of the new model in terms of cpu time or memory storage. In this section, the improved computational performance of the fourth-order model is demonstrated by example.

As mentioned, the computational advantage of the new fourth-order model is a decrease in dispersive errors. However, the fourth-order model also possesses three computational disadvantages. The first computational disadvantage is the increased memory storage per cell. In Section V it was noted that the fourth-order TLM model requires double the memory storage of the original algorithm per cell. The second computational disadvantage is the increased computation required

per cell, due to increased algorithmic complexity (more multiplications and additions). Our simulations indicate that the new fourth-order model requires approximately 2.5 times more cpu time per cell as compared to the original model (a similar comparison for the equivalent finite-difference algorithms has not been performed). The third computational disadvantage is that the fourth-order model possesses a smaller maximum allowable time step (see (8) and (9)) as compared to the original model [7]. Therefore, more time steps are required to achieve the same effective duration of computation. The following examples illustrate that the computational advantage of increased accuracy allows for sufficiently coarse discretization such that the three computational disadvantages discussed above are offset.

Consider an arbitrary two-dimensional problem of a given spatial size that requires simulation for a given duration of time. In this example, the suggestion made in Section IV is followed, and the free space region is normalized to possess a stub value of $Y_0 = 13.067$ (which would usually correspond to a relative permittivity ε_r =4.0, see (10)). This specific renormalization value is selected as an example and should not be considered as optimal. For this stub value, the maximum allowable time step permitted by the fourth-order model is 2.31 times smaller than that permitted by the original model operated at the upper limit of stability. Consider the operation of the second-order algorithm such that the spatial discretization (for the highest desired output frequency) is 15 $\Delta l/\lambda$. For this discretization, the original model provides an E_d value of 0.1845. To obtain the same value of E_d, the new fourth-order algorithm requires a discretization of only $5.64\Delta l/\lambda$. For a two-dimensional region, the original model requires $(15.0/5.64)^2 = 7.07$ times more cells to achieve the same accuracy. Taking into account that the fourth-order model requires twice as much memory storage, the new fourth-order model requires 3.5 times less memory than the second-order algorithm. In terms of cpu time, taking into account that the fourth-order algorithm requires $2.31 \times 2.5 = 5.8$ times more cpu time per cell (due to the restricted Δt requirement and the increase in algorithmic complexity), the fourth-order algorithm requires approximately 1.2 times less cpu time than the second-order algorithm. Only a slight advantage is realized for this example in terms of cpu time, but a significant advantage in memory storage.

Now consider a problem involving a free-space region and a dielectric region with ε_r =10. The same order of accuracy is desired in the dielectric region as was obtained in the free-space region of the above problem (i.e., E_d =0.1845). To achieve this accuracy within the dielectric medium with the original model requires a discretization 24.9 $\Delta l/\lambda$. To achieve the same accuracy, the fourth-order algorithm requires a discretization of 6.98 $\Delta l/\lambda$. Over a two-dimensional region 12.7 times more cells are required by the second-order algorithm to achieve the same accuracy provided by the fourth-order algorithm. Therefore, the fourth-order algorithm requires 6.4 times less memory and 2.2 times less cpu time than the second-order algorithm for equivalent accuracy. Both examples indicate a computational advantage provided by the new fourth-order model.

VII. Discussion / Conclusion

In this paper a spatially fourth-order version of the original two-dimensional TLM algorithm has been presented. The fundamental accuracy of the spatial approximation has been increased from second to fourth-order. The same improvement is possible for the hexagonal [4] and spatially weighted TLM models [5] to obtain spatially fourth-order versions. The accuracy of the temporal discretization remains second-order. The concept of a stability criteria has been introduced to the TLM method and is based on the permissible values for the stub admittance Y_0.

As discussed in Section III, the fourth-order TLM model is constructed with elemental transmission lines with negative characteristic impedances. Although physically unrealistic, these negative impedance transmission lines are required to obtain the appropriate weighting present in the equivalent finite-difference algorithm. The negative impedance transmission lines could have been avoided through the use of bi-directional impedance inverters (which would require infinite bandwidth) to interface lines 1–4 and 9 with lines 5–8 and 10. The bi-directional impedance inverters would also be physically unrealistic. These aspects of the fourth-order model should not be a cause for concern since TLM models are used as a simulation tool and their physical realizability is not an issue.

Some unique properties of the fourth-order model have emerged. For the modelling of dielectric material, the dispersive errors associated with the algorithm decrease for moderate ε_r (also true for the equivalent finite-difference algorithm). The improved dispersive properties of the fourth-order models make them attractive candidates for the analysis of electrically large (and inhomogeneous) problems.

References

[1] W. J. R. Hoefer, "The transmission-line matrix method—Theory and applications." *IEEE Trans. Microwave Theory Tech.*, vol. MTT-33, no. 10, pp. 882–893, Oct. 1985.

[2] ——, "The transmission-line matrix (TLM) method," in *Numerical Techniques for Microwave and Millimeter Wave Passive Structures*, T. Itoh, Ed. New York: Wiley, 1989.

[3] L. Lapidus and G. F. Pinder, *Numerical Solution of Partial Differential Equations in Science and Engineerin.* New York:Wiley, 1982.

[4] N. R. S. Simons and A. Sebak, "New transmission-line matrix node for two-dimensional electromagnetic field problems," *Canadian J. Phys.*, vol. 69, no. 11, pp. 1388–1398, 1991.

[5] ——, "Spatially weighted numerical models for the two-dimensional wave equations: FD algorithm and synthesis of the equivalent TLM model," *Int. J. Numerical Modelling*, vol. 6, pp. 47–65, 1993.

[6] N. R. S. Simons and E. Bridges, "Equivalence of propagation characteristics for the transmission-line matrix an finite-difference time-domain methods in two dimensions," *IEEE Trans. Microwave Theory Tech.*, vol. MTT-39, pp. 243–267, 1991.

[7] P. B. Johns and R. L. Beurle, "Numerical solution of two dimensional scattering problems using a transmission line matrix," *Proc. Inst. Elec. Eng.*, vol. 118, no. 9, pp. 1203–1208, Nov. 1971.

[8] J. Fang and K. K. Mei, "A higher order finite difference scheme for the solution of Maxwell's Equations in the time domain," in*Proc. 1989 URSI Radio Science Meeting*, San Jose, CA, 1989.

[9] T. Deveze, L. Beaulieu, and W. Tabbara, "A fourth order scheme for the FDTD algorithm applied to Maxwell's equations," in *Proc. 1993 IEEE AP-S Int. Symp.*, 1992, Chicago IL, pp. 346–349.

[10] R. Vichnevetsky and J. B. Bowles, *Fourier Analysis of Numerical Approximations of Hyperbolic Equations.* Philadelphia: SIAM, 1982.

[11] G. O. O'Brien, M. A. Hyman, and S. Kaplan, "A study of the numerical solution of partial differential equations," *J. Mathemat. Phys.*, vol. 29, p. 223, 1950.

[12] K. S. Yee, "Numerical solution of initial boundary value problems involving Maxwell's Equations in isotropic media," *IEEE Trans. Antennas Propagat.,* vol. AP-14, no. 3, pp. 302–307, May 1966.
[13] A. Taflove and K. R. Umashankar, "Review of FD-TD numerical modelling of electromagnetic wave scattering and radar cross section," *Proc. IEEE,* vol. 77, no. 5, pp. 682–699, May 1989.
[14] C. R. Brewitt-Taylor and P. B. Johns, "On the construction an numerical solution of transmission-line and lumped network models of Maxwell's Equations," *Int. J. Numerical Methods in Engineering,* vol. 15, pp. 13–30, 1980.
[15] P. B. Johns, "On the relationship between TLM and finite-difference methods for Maxwell's Equations," *IEEE Trans. Microwave Theory Tech.,* vol. MTT-35, no. 1, pp. 60–61, 1987.
[16] N. R. S. Simons, "Application of the TLM method to open region field problems," M.Sc. thesis, University of Manitoba, 1990.
[17] Z. Chen, M. M. Ney, and W. J. R. Hoefer, "A new finite-difference time-domain formulation and its equivalence with the TLM Symmetric condensed node," *IEEE Trans. Microwave Theory Tech.,* vol. MTT-39, pp. 2160–2169, 1991, and, M. Celuch-Marcysiak and W. K. Gwarek, Comments on "A new finite-difference time-domain formulation and its equivalence with the TLM symmetrical condensed node," *IEEE Trans. Microwave Theory Tech.,* vol. MTT-41, no. 1, pp. 168–172, Jan. 1993.

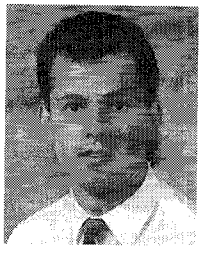

Neil R. S. Simons received the B.Sc. degree (with distinction) and M.Sc. degree from the University of Manitoba, Winnipeg, MB, Canada, in 1987 and 1990, respectively, both in electrical engineering. From 1987 to 1989 he was with Quantic Laboratories, Winnipeg, working on problems related to transmission-line effects on printed circuit boards. He is currently a Ph.D. student at the University of Manitoba, and is also employed with InfoMagnetics Technologies Corporation, Winnipeg. His primary research interst is the numerical solution of electromagnetic field problems.

Abdel-Razik Sebak (S'81–M'84–SM'92) received the B.Sc. degree (with Honors) in electrical engineering from Cairo University, Egypt, in 1976 and the B.Sc. degree in applied mathematics from Ein Shams University, Egypt, in 1978. He received the M.Eng. and Ph.D. degrees from the University of Manitoba, Winnipeg, MB, Canada, in 1982 and 1984, respectively, both in electrical engineering.

From 1984 to 1986, he was with the Canadian Marconi Company, Kanata, Ontario, working on the design of microstrip phased array antennas. He is currently an associate professor of electrical and computer engineering, the University of Manitoba. His current research interests include computational electromagnetics, integrated antennas, electromagnetic theory, detection of subsurface conducting objects and electromagnetic interference.

Dr. Sebak received the 1992 University of Manitoba Merit Award for outstanding Teaching and Research. He has served as Chairman (1991–92) of the joint IEEE AP/MTT/VT Winnipeg Chapter. He received, as Chapter Chairman, the 1992 IEEE Antennas and Propagation Society Best Chapter Award.